

# An Immunosuppressive Antibody–Drug Conjugate

Rongsheng E. Wang,<sup>†,⊥</sup> Tao Liu,<sup>†,⊥</sup> Ying Wang,<sup>§</sup> Yu Cao,<sup>†</sup> Jintang Du,<sup>§</sup> Xiaozhou Luo,<sup>†</sup> Vishal Deshmukh,<sup>†</sup> Chan Hyuk Kim,<sup>§</sup> Brian R. Lawson,<sup>§,‡</sup> Matthew S. Tremblay,<sup>§</sup> Travis S. Young,<sup>§</sup> Stephanie A. Kazane,<sup>\*,§</sup> Feng Wang,<sup>\*,§</sup> and Peter G. Schultz<sup>\*,†,§</sup>

<sup>†</sup>Department of Chemistry and the Skaggs Institute for Chemical Biology and <sup>‡</sup>Department of Immunology and Microbial Science, The Scripps Research Institute, La Jolla, California 92037, United States

<sup>§</sup>California Institute for Biomedical Research (Calibr), La Jolla, California 92037, United States

## Supporting Information

**ABSTRACT:** We have developed a novel antibody–drug conjugate (ADC) that can selectively deliver the Lck inhibitor dasatinib to human T lymphocytes. This ADC is based on a humanized antibody that selectively binds with high affinity to CXCR4, an antigen that is selectively expressed on hematopoietic cells. The resulting dasatinib–antibody conjugate suppresses T-cell-receptor (TCR)-mediated T-cell activation and cytokine expression with low nM EC<sub>50</sub> and has minimal effects on cell viability. This ADC may lead to a new class of selective immunosuppressive drugs with improved safety and extend the ADC strategy to the targeted delivery of kinase inhibitors for indications beyond oncology.

Antibody–drug conjugates (ADCs) are an emerging class of immunotherapeutic agents that allow the targeted delivery of potent cytotoxic agents to cancer cells.<sup>1</sup> A number of toxins such as doxorubicin, auristatin, and calicheamicin have been conjugated to monoclonal antibodies that selectively bind various antigens overexpressed in cancers.<sup>2–4</sup> Examples include trastuzumab-DM1 and brentuximab-vedotin, which were recently FDA approved for the treatment of HER2-overexpressing breast cancer and Hodgkin's lymphoma, respectively.<sup>1</sup> Despite substantial progress in the development of ADCs in oncology, few applications using noncytotoxic agents outside the field of oncology have been reported.<sup>5</sup> To this end, we asked whether an ADC approach can be applied to other classes of small molecule drugs, in particular, kinase inhibitors, for the treatment of autoimmune and inflammatory diseases.<sup>6,7</sup> Unfortunately, many kinase inhibitors, including those currently in clinical use, suffer from a lack of selectivity for related kinase family members, which leads to off-target toxicity. This low therapeutic index has largely limited kinase inhibitors to the treatment of cancer despite their considerable potential in other disease settings.<sup>8,9</sup> For example, dasatinib, which is used clinically for the treatment of BCR-ABL-dependent chronic myelogenous leukemia, is also a potent inhibitor (IC<sub>50</sub> < 1 nM) of other Src-family kinases. These include Lck and Fyn,<sup>10,11</sup> which play key roles in T-cell receptor (TCR) signaling by phosphorylating and activating downstream kinases including ZAP70.<sup>12,13</sup> Despite its promise for the treatment of T-cell mediated immune disorders, the lack of selectivity of dasatinib leads to severe side effects including pleural effusions and cardiovascular dysfunction, as

well as dermatologic toxicity,<sup>14</sup> which collectively undermine its development as an immunosuppressive agent. Given its lack of selectivity, but highly potent activity in inhibiting T-cell activation, we asked whether we could selectively target dasatinib to T cells as an ADC and thereby improve its therapeutic index.

To selectively deliver dasatinib to T lymphocytes, we considered a number of antibodies that selectively bind T-cell antigens including CD3, CD4, CD70, and CD184 (CXCR4). Among these, CXCR4 is highly expressed on the surface of human T cells (Figure S1)<sup>15,16</sup> but has minimal to no expression on nonhematopoietic cells as well as resting neutrophils.<sup>16–18</sup> Although CXCR4 is also expressed on hematopoietic stem cells (HSCs), B-cells, and monocytes, delivery of dasatinib to these cells is not likely to cause serious side effects.<sup>15,16,19,20</sup> Moreover, it has been demonstrated that antibodies that bind CXCR4 are efficiently internalized, and their antagonism of CXCR4-signaling is not associated with significant adverse clinical effects,<sup>21–24</sup> which suggests that they are excellent candidates for conjugation with dasatinib.

We recently developed an anti-CXCR4 antibody that specifically binds to CXCR4 with high affinity by grafting a CXCR4 peptide antagonist into the extended complementarity determining region (CDR) of the bovine antibody (BLV1H12) scaffold.<sup>25</sup> However, to use this antibody in an ADC, we needed to first generate a humanized version to avoid a neutralizing immune response upon chronic administration. To this end, we grafted the long CDR3H of the bovine anti-CXCR4 antibody<sup>25</sup> into CDR3H of trastuzumab, an antibody with minimal immunogenicity in humans (Figure 1A). The long CDR3H of the bovine anti-CXCR4 consists of a disulfide cross-linked  $\beta$ -hairpin peptide that specifically binds the ligand binding pocket of CXCR4. The CXCR4 targeting hairpin peptide was inserted into CDR3H between Arg98 and Asp108, replacing the original Trp99–Met107 loop in CDR3H of trastuzumab, to afford the humanized antibody HLCX (Figure 1A,B). HLCX was transiently expressed in HEK 293F cells and purified by Protein G chromatography with a final yield of ~5 mg/L. Denaturing SDS-PAGE gel electrophoresis demonstrated that the antibody was >90% pure and resolved into bands of ~150 kDa (nonreducing conditions, full length IgG) and ~50 and ~25 kDa (reducing conditions, heavy and light chains, respectively) (Figure S2A). Further analysis of HLCX by electrospray-

Received: January 19, 2015

Published: February 20, 2015



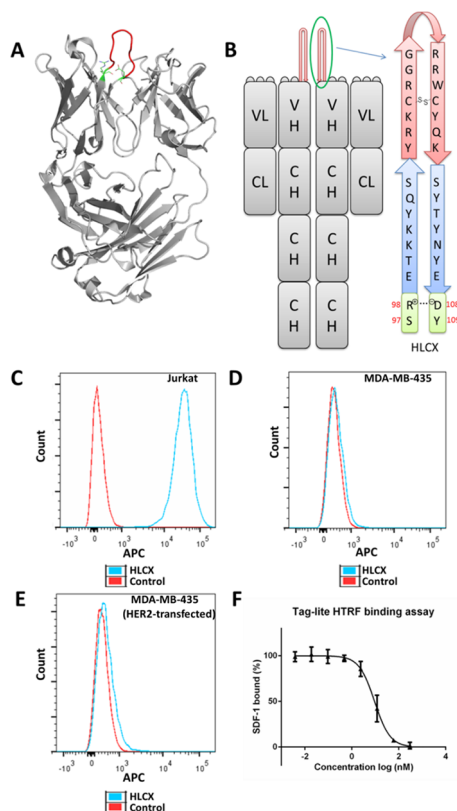


**Figure 1.** (A) Crystal structure of trastuzumab Fab (PDB code: 1N8Z). CDR3H of trastuzumab is labeled in red, and the side chains of Arg98 and Asp108 are marked. (B) A graphic representation of anti-CXCR4 antibody (HLCX) design. A disulfide cross-linked CXCR4-specific  $\beta$ -hairpin peptide (red) stabilized by an antiparallel  $\beta$ -stranded linker (blue) was engineered onto the CDR3H loop of trastuzumab. Flow cytometry histogram showing the binding of HLCX to (C) CXCR4-expressing Jurkat T cells, (D) CXCR4-negative MDA-MB435 cells, and (E) HER2-transfected MDA-MB435 cells. (F) Measurement of binding affinity between HLCX and human CXCR4 by a Tag-lite HTRF binding assay.

ionization–mass spectrometry (ESI–MS) indicated the expected molecular weight (Figure S2B).

We next examined the binding of HLCX to cell-surface CXCR4 by flow cytometry. Incubation of 10 nM HLCX with Jurkat T cells (CXCR4<sup>high</sup>)<sup>24</sup> resulted in a peak shift of 96.2% by flow cytometry analysis (Figure 1C). In contrast, incubation of HLCX with MDA-MB-435 cells (CXCR4<sup>neg</sup>)<sup>26</sup> did not result in any shift (Figure 1D), which indicates that HLCX binds human CXCR4 selectively. Given that HLCX was derived from the trastuzumab scaffold, we also tested the binding of HLCX to HER2-transfected MDA-MB-435 cells<sup>27</sup> (Figure S3). A minimal peak shift (Figure 1E) demonstrated that fusion into the CDR3H of trastuzumab abrogates binding to its cognate antigen.<sup>28</sup> To further characterize the binding profile of HLCX, a series of flow cytometry analyses were performed on additional cell lines expressing different levels of CXCR4 (Figure S4), which further confirmed that HLCX is a selective antibody toward CXCR4. We then directly measured the binding affinity of HLCX to human CXCR4 using Tag-lite homogeneous time-resolved fluorescence (HTRF) as described previously.<sup>25,29</sup> The  $K_d$  value for HLCX was determined to be  $2.1 \pm 0.2$  nM (Figure 1F).

Given its selectivity and high affinity, we next examined the internalization of HLCX by human T cells, as this is required for efficient delivery of the drug to its intracellular target by an ADC.

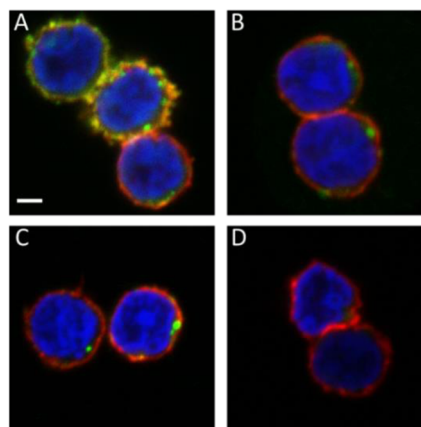
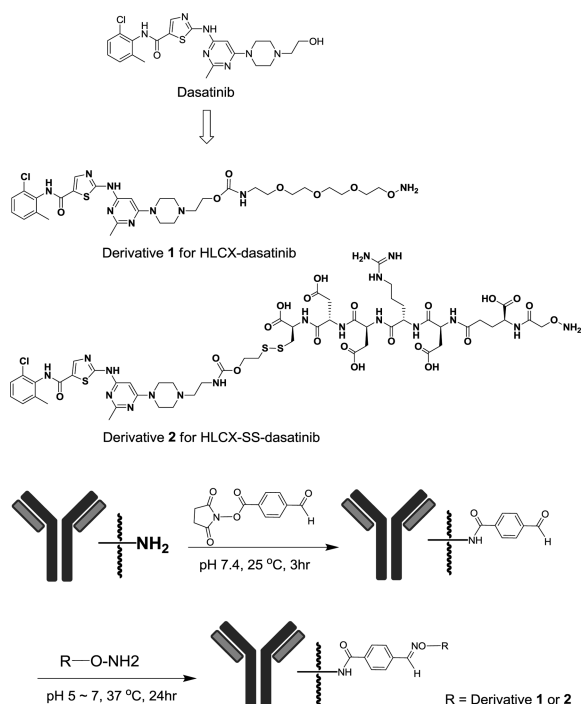


**Figure 2.** Confocal microscopy of internalization of anti-CXCR4 antibodies labeled with Alexa Fluor 488. Human T cells were incubated with 50 nM HLCX-AF488 for 30 min at (A) 37 °C or (B) 4 °C, (C) 50 nM 12G5-AF488 at 37 °C, or (D) 50 nM HLCX-AF488 at 37 °C in the presence of 1  $\mu$ M HLCX. Cells were then fixed, stained with Hoechst dye (blue, nucleus), Alexa Fluor 594-conjugated wheat germ agglutinin (red, membrane), and imaged with a Leica 710 confocal microscope. Bar = 2  $\mu$ m.

The antibody was conjugated with Alexa Fluor 488 (AF488) by reacting lysyl amino groups with AF488-NHS ester to achieve a drug-to-antibody ratio (DAR) of  $\sim 4$  (Figure S5). Confocal microscopic analysis was used to determine the efficiency of internalization of the antibody into human T cells (Figure 2). For comparison, a common anti-CXCR4 commercial clone (12G5) was also conjugated to AF488 at a similar DAR (Figure S6). As shown in Figure 2, panel A, HLCX-AF488 (green spots) was observed in the cytoplasm of T cells within 30 min at 37 °C, which indicates efficient endocytosis. Internalization was inhibited at 4 °C (Figure 2B) or in the presence of 20-fold excess of unconjugated HLCX (Figure 2D), which indicates that internalization is CXCR4-mediated. In contrast, a lower amount of 12G5-AF488 was observed inside the cytoplasm, which suggests that 12G5 is internalized less efficiently than HLCX (Figure 2C). It is known that internalization efficiency depends on binding epitopes.<sup>30</sup> The long CDR3H of HLCX targets the ligand binding pocket of CXCR4,<sup>25</sup> which may contribute to its high internalization efficiency. Taken together, these results suggest that HLCX is an excellent candidate for CXCR4-targeted delivery.

Next, we designed and synthesized dasatinib-linker derivatives for conjugation with HLCX (Scheme 1). Structure–activity relationship and modeling studies have indicated that the hydroxyl moiety of dasatinib is not essential for activity.<sup>12,13</sup> Therefore, we installed a linker for conjugation to the antibody by modifying the hydroxyl group of dasatinib with p-nitrophenyl chloroformate, followed by carbamylation with a tetra-polyethylene glycol (PEG) linker bearing a protected aminoxy moiety for conjugation (Scheme S1). The resulting intermediate was readily deprotected to afford the desired derivative **1** with a noncleavable linker (Scheme 1). An in vitro kinase inhibition assay with Lck (Figure S9) confirmed that this derivative had a similar potency as the parent compound ( $EC_{50} = 65.2 \pm 5.1$  pM for **1** vs  $21.6 \pm 1.9$  pM for dasatinib). Since it has been reported that cleavable linkers may enhance the efficacy of antibody drug conjugates,<sup>31–33</sup> we also prepared a dasatinib disulfide-cleavable linker **2**, which consists of a peptide spacer unit to increase solubility,<sup>31,33</sup> an alkoxyamine group for conjugation, and a

## Scheme 1. Synthesis of HLCX-Based Antibody Drug Conjugates



disulfide bond to be selectively cleaved inside cells to release the amino-substituted dasatinib derivative (which has a two-fold higher  $K_d$  relative to dasatinib (Figure S10)) (Scheme S2).<sup>34</sup>

Next we developed a versatile two-step coupling procedure for the synthesis of the ADC (Scheme 1). The first step involved nonspecific derivatization of the lysyl amino groups of the antibody with S-4FB linker (Solulink), followed by desalting chromatography to introduce aryl aldehydes in a stoichiometry of about three aldehydes to one antibody. The modified antibody was then reacted with a 30-fold excess of amino-oxo-derived dasatinib linker compounds at 37 °C for 24 h in >95% yield as determined by ESI-MS. The resulting antibody conjugates with the noncleavable linker and disulfide-cleavable linkers, designated as HLCX-dasatinib and HLCX-SS-dasatinib, respectively, were then purified by size exclusion chromatography (Superdex-200). SDS-PAGE (Figure S7) and ESI-MS (Figure S8) showed that the dasatinib ADCs were >90% pure with a DAR of ~3 and have the expected molecular weights.

To evaluate their *in vitro* activity, the two ADCs were incubated with freshly isolated human T cells that were stimulated with anti-CD3/anti-CD28 antibodies.<sup>11</sup> T cells express CD69 surface antigen during early stage activation and gradually express an increasing amount of CD25 as stimulation continues.<sup>35</sup> Simultaneously, cytokines such as IL-2, TNF $\alpha$ , and IFN $\gamma$  are secreted by T cells to promote their proliferation as well as help activate other accessory cells.<sup>11</sup> Analysis by flow cytometry (Figure S11) and ELISA (Figure 3A) showed that both ADCs significantly inhibited CD69/CD25 expression and suppressed cytokine secretion; HLCX-SS-dasatinib was efficacious at concentrations as low as 8 nM. In contrast, the unconjugated HLCX antibody displayed minimal effects ( $EC_{50}$  > 200 nM). HLCX-SS-dasatinib was about two-fold more potent than HLCX-dasatinib in suppressing IL-2 ( $EC_{50}$  = 12.7  $\pm$  5.8 nM vs 32.1  $\pm$  11.3 nM), TNF $\alpha$  ( $EC_{50}$  = 26.3  $\pm$  9.0 nM vs 66.1  $\pm$  30.5 nM), and IFN $\gamma$  ( $EC_{50}$  = 58.7  $\pm$  28.6 nM vs 123.5  $\pm$  43.3 nM)

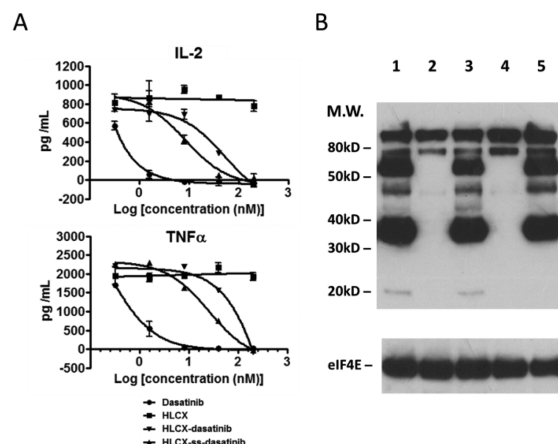


**Figure 3.** Inhibition of TCR-mediated activation of human T cells. (A) Inhibition of cytokine secretion (Interleukin-2 and TNF $\alpha$ ) of  $\alpha$ CD3/ $\alpha$ CD28-activated T cells by dasatinib (positive control,  $EC_{50}$ s  $\approx$  0.2–1 nM), unconjugated HLCX (negative control), HLCX-dasatinib non-cleavable ADC ( $EC_{50}$  for IL-2, 32.1  $\pm$  11.3 nM;  $EC_{50}$  for TNF $\alpha$ , 66.1  $\pm$  30.5 nM), and HLCX-SS-dasatinib cleavable ADC ( $EC_{50}$  for IL-2, 12.7  $\pm$  5.8 nM;  $EC_{50}$  for TNF $\alpha$ , 26.3  $\pm$  9.0 nM). (B) Western blot for TCR complex signal transduction. T cells were stimulated without compound treatment (lane 1) or in the presence of 100 nM dasatinib (lane 2), HLCX (lane 3), HLCX-SS-dasatinib ADC (lane 4), or trastuzumab-SS-dasatinib (lane 5) at 37 °C, then immediately lysed. Proteins were separated on SDS-PAGE, transferred to PVDF membrane, and probed with pan antiphosphotyrosine antibody. eIF4E served as the loading control.

(Figure 3A, Figure S12). This relatively small difference in activity could be due to differences in the efficiencies of internalization and/or drug release, differences in the potencies of the dasatinib analogues, or differences in drug residence times in the cell. However, to ensure that the increased potency of HLCX-SS-dasatinib is not due to premature release of dasatinib outside the cells, we conjugated the disulfide cleavable dasatinib to a control antibody, trastuzumab, in a similar manner as above and evaluated its activity in cytokine secretion assays. Trastuzumab-SS-dasatinib showed negligible effects at concentrations up to 200 nM, whereas dasatinib itself completely suppressed cytokine secretion ( $EC_{50}$ s  $\approx$  0.2–1.6 nM) (Figure S13). Additionally, to rule out the possibility that the observed immunosuppression is due to an unexpected cytotoxic activity, the viability of T cells was also measured using CellTiter Glo (Figure S12B). As compared to untreated T cells, the activated T cells did not show any significant loss in viability after incubation with either dasatinib or ADCs at concentrations up to 200 nM.

Although suppression of T-cell activation by the dasatinib-ADCs is CXCR4-dependent, we wanted to confirm that the underlying activity is due to inhibition of Lck by dasatinib. To this end, Western blot analysis was carried out to examine the phosphorylation of downstream kinases during TCR-induced T-cell activation (Figure 3B). As shown in lane 1, TCR activation occurs after T cells are cross-linked with OKT3 at 37 °C. Dasatinib, as a positive control, efficiently blocked Lck-mediated phosphorylation of tyrosine on multiple kinases including ZAP70 (lane 2). As indicated in lane 4, HLCX-SS-dasatinib (100 nM) also blocked Lck signaling, whereas HLCX itself (lane 3) and trastuzumab-SS-dasatinib (negative control) displayed negligible effects (lane 5). Taken together, suppression of T-cell activation by HLCX-SS-dasatinib ADC is both antibody and small-molecule dependent, which suggests that a relatively



promiscuous kinase inhibitor can be successfully delivered to T cells by the anti-CXCR4 antibody HLCX.

In conclusion, we have developed a novel ADC using a humanized CXCR4-specific IgG with an elongated CDR3H that was nonspecifically conjugated to dasatinib derivatives via both cleavable and noncleavable linkers. These ADCs are able to selectively deliver dasatinib to human T cells with excellent in vitro immunosuppressive activity, which is likely in part due to the high potency of the parent kinase inhibitor. The in vivo efficacy of the anti-CXCR4-dasatinib conjugate was not evaluated in rodents due to significant differences in CXCR4 expression in rodent versus human T cells.<sup>36</sup> Further evaluation of the conjugates in a more advanced surrogate model (e.g., cynomolgus monkeys) will be required to determine its therapeutic potential as a tissue-targeted immunosuppressive drug with the potential for improved efficacy and safety. In addition, we are comparing the activity of these ADCs with ADCs site-specifically modified with dasatinib.<sup>27</sup> Finally, this work suggests that the ADC strategy has applicability beyond the field of oncology as a route to improve the selectivity of highly potent biologically active small molecules including kinase inhibitors.

## ■ ASSOCIATED CONTENT

### ■ Supporting Information

Experimental details and supporting figures. This material is available free of charge via the Internet at <http://pubs.acs.org>.

## ■ AUTHOR INFORMATION

### Corresponding Authors

\*spinkerton@calibr.org

\*fwang@calibr.org

\*schultz@scripps.edu

### Author Contributions

<sup>†</sup>These authors contributed equally.

### Notes

The authors declare no competing financial interest.

## ■ ACKNOWLEDGMENTS

We thank Dr. Aaron Pearson (TSRI) for help on solid-phase synthesis, and Dr. Damien Bresson (Ambrx, Inc.) for helpful discussions. This work was supported by funding from Calibr and National Institutes of Health under award 2 R01 GM097206-05.

## ■ REFERENCES

- (1) Sassoon, I.; Blanc, V. *Methods Mol. Biol.* **2013**, 1045, 1.
- (2) Sutherland, M. S.; Sanderson, R. J.; Gordon, K. A.; Andreyka, J.; Cerveny, C. G.; Yu, C.; Lewis, T. S.; Meyer, D. L.; Zabinski, R. F.; Doronina, S. O.; Senter, P. D.; Law, C. L.; Wahl, A. F. *J. Biol. Chem.* **2006**, 281, 10540.
- (3) Dubowchik, G. M.; Firestone, R. A.; Padilla, L.; Willner, D.; Hofstead, S. J.; Mosure, K.; Knipe, J. O.; Lasch, S. J.; Trail, P. A. *Bioconjugate Chem.* **2002**, 13, 855.
- (4) Ricart, A. D. *Clin. Cancer Res.* **2011**, 17, 6417.
- (5) Graversen, J. H.; Svendsen, P.; Dagnaes-Hansen, F.; Dal, J.; Anton, G.; Etzerodt, A.; Petersen, M. D.; Christensen, P. A.; Miller, H. J.; Moestrup, S. K. *Mol. Ther.* **2012**, 20, 1550.
- (6) Bhagwat, S. S. *Purinergic Signal* **2009**, 5, 107.
- (7) Patterson, H.; Nibbs, R.; McInnes, I.; Siebert, S. *Clin. Exp. Immunol.* **2014**, 176, 1.
- (8) Adis Editorial. *Drugs R&D* **2010**, 10, 271.
- (9) McCormack, P. L. *Drugs* **2015**, 75, 129.
- (10) Blake, S.; Hughes, T. P.; Mayrhofer, G.; Lyons, A. B. *Clin. Immunol.* **2008**, 127, 330.
- (11) Schade, A. E.; Schieven, G. L.; Townsend, R.; Jankowska, A. M.; Susulic, V.; Zhang, R.; Szpurka, H.; Maciejewski, J. P. *Blood* **2008**, 111, 1366.
- (12) Das, J.; Chen, P.; Norris, D.; Padmanabha, R.; Lin, J.; Moquin, R. V.; Shen, Z.; Cook, L. S.; Doweiko, A. M.; Pitt, S.; Pang, S.; Shen, D. R.; Fang, Q.; de Fex, H. F.; McIntyre, K. W.; Shuster, D. J.; Gillooly, K. M.; Behnia, K.; Schieven, G. L.; Wityak, J.; Barrish, J. C. *J. Med. Chem.* **2006**, 49, 6819.
- (13) Lombardo, L. J.; Lee, F. Y.; Chen, P.; Norris, D.; Barrish, J. C.; Behnia, K.; Castaneda, S.; Cornelius, L. A.; Das, J.; Doweiko, A. M.; Fairchild, C.; Hunt, J. T.; Inigo, I.; Johnston, K.; Kamath, A.; Kan, D.; Klei, H.; Marathe, P.; Pang, S.; Peterson, R.; Pitt, S.; Schieven, G. L.; Schmidt, R. J.; Tokarski, J.; Wen, M. L.; Wityak, J.; Borzilleri, R. M. *J. Med. Chem.* **2004**, 47, 6658.
- (14) Giles, F. J.; O'Dwyer, M.; Swords, R. *Leukemia* **2009**, 23, 1698.
- (15) Bleul, C. C.; Wu, L.; Hoxie, J. A.; Springer, T. A.; Mackay, C. R. *Proc. Natl. Acad. Sci. U. S. A.* **1997**, 94, 1925.
- (16) Hori, T.; Sakaida, H.; Sato, A.; Nakajima, T.; Shida, H.; Yoshie, O.; Uchiyama, T. *J. Immunol.* **1998**, 160, 180.
- (17) Nagase, H.; Miyamasu, M.; Yamaguchi, M.; Imanishi, M.; Tsuno, N. H.; Matsushima, K.; Yamamoto, K.; Morita, Y.; Hirai, K. *Leukocyte Biol.* **2002**, 71, 711.
- (18) Weisel, K. C.; Bautz, F.; Seitz, G.; Yildirim, S.; Kanz, L.; Mohle, R. *Mediators Inflammation* **2009**, 2009, 790174.
- (19) Lee, B.; Sharron, M.; Montaner, L. J.; Weissman, D.; Doms, R. W. *Proc. Natl. Acad. Sci. U. S. A.* **1999**, 96, 5215.
- (20) Bleul, C. C.; Schultze, J. L.; Springer, T. A. *J. Exp. Med.* **1998**, 187, 753.
- (21) Signoret, N.; Oldridge, J.; Pelchen-Matthews, A.; Klasse, P. J.; Tran, T.; Brass, L. F.; Rosenkilde, M. M.; Schwartz, T. W.; Holmes, W.; Dallas, W.; Luther, M. A.; Wells, T. N.; Hoxie, J. A.; Marsh, M. J. *Cell Biol.* **1997**, 139, 651.
- (22) Kumar, A.; Humphreys, T. D.; Kremer, K. N.; Bramati, P. S.; Bradfield, L.; Edgar, C. E.; Hedin, K. E. *Immunity* **2006**, 25, 213.
- (23) Kohler, R. E.; Comerford, I.; Townley, S.; Haylock-Jacobs, S.; Clark-Lewis, I.; McColl, S. R. *Brain Pathol.* **2008**, 18, 504.
- (24) Hesselgesser, J.; Liang, M.; Hoxie, J.; Greenberg, M.; Brass, L. F.; Orsini, M. J.; Taub, D.; Horuk, R. *J. Immunol.* **1998**, 160, 877.
- (25) Liu, T.; Liu, Y.; Wang, Y.; Hull, M.; Schultz, P. G.; Wang, F. *J. Am. Chem. Soc.* **2014**, 136, 10557.
- (26) Liang, Z.; Wu, T.; Lou, H.; Yu, X.; Taichman, R. S.; Lau, S. K.; Nie, S.; Umbreit, J.; Shim, H. *Cancer Res.* **2004**, 64, 4302.
- (27) Axup, J. Y.; Bajjuri, K. M.; Ritland, M.; Hutchins, B. M.; Kim, C. H.; Kazane, S. A.; Halder, R.; Forsyth, J. S.; Santidrian, A. F.; Stafin, K.; Lu, Y.; Tran, H.; Seller, A. J.; Biroc, S. L.; Szydlak, A.; Pinkstaff, J. K.; Tian, F.; Sinha, S. C.; Felding-Habermann, B.; Smider, V. V.; Schultz, P. G. *Proc. Natl. Acad. Sci. U. S. A.* **2012**, 109, 16101.
- (28) Zhang, Y.; Liu, Y.; Wang, Y.; Schultz, P. G.; Wang, F. *J. Am. Chem. Soc.* **2015**, 137, 38.
- (29) Lazareno, S.; Birdsall, N. J. *Br. J. Pharmacol.* **1993**, 109, 1110.
- (30) Terp, M. G.; Olesen, K. A.; Arnspang, E. C.; Lund, R. R.; Lagerholm, B. C.; Ditzel, H. J.; Leth-Larsen, R. *J. Immunol.* **2013**, 191, 4165.
- (31) Leamon, C. P.; Reddy, J. A.; Vlahov, I. R.; Kleindl, P. J.; Vetzal, M.; Westrick, E. *Bioconjugate Chem.* **2006**, 17, 1226.
- (32) Polson, A. G.; Calemene-Fenaux, J.; Chan, P.; Chang, W.; Christensen, E.; Clark, S.; de Sauvage, F. J.; Eaton, D.; Elkins, K.; Elliott, J. M.; Frantz, G.; Fujii, R. N.; Gray, A.; Harden, K.; Ingle, G. S.; Kljavin, N. M.; Koepfen, H.; Nelson, C.; Prabhu, S.; Raab, H.; Ross, S.; Slaga, D. S.; Stephan, J. P.; Scales, S. J.; Spencer, S. D.; Vandlen, R.; Wranik, B.; Yu, S. F.; Zheng, B.; Ebens, A. *Cancer Res.* **2009**, 69, 2358.
- (33) Vlahov, I. R.; Leamon, C. P. *Bioconjugate Chem.* **2012**, 23, 1357.
- (34) Fischer, J. J.; Dalhoff, C.; Schrey, A. K.; Graebner, O. Y.; Michaelis, S.; Andrich, K.; Gliniski, M.; Kroll, F.; Sefkow, M.; Dreger, M.; Koester, H. *J. Proteomics* **2011**, 75, 160.
- (35) Arva, E.; Andersson, B. *Scand. J. Immunol.* **1999**, 49, 237.
- (36) Schabath, R.; Muller, G.; Schubel, A.; Kremmer, E.; Lipp, M.; Forster, R. *J. Leukocyte Biol.* **1999**, 66, 996.